UIT Report Vol. 14, No. 1, pp. 25~29, 1983　　　　연구논문집 제14권 제 1 호 pp. 25~29, 1983

Analysis of Anisotropy in Carbon Fibre Reinforced Plastic Materials during Bending

Yum Young Jin
Dept. of Mechanical Engineering
(Received October 30, 1982)

〈**Abstract**〉

The location of neutral axis in carbon/epoxy composites has been analysed theoretically with the flatwise multilayered laminates and edgewise laminates.

The modulus measurements of unidirectional [0°] and [90°] laminae were shown to be $(E_t)_{0°} = 1.31(E_c)_{0°}$ and $(E_t)_{90°} = 0.93(E_c)_{90°}$ respectively.

Experimental determination of the neutral axis was made from the strain measurements.

The comparison was made between these two results and the percentage deviation of h_t/h was found to be less than 3% for [0°/90°/90°/0°] [0°/90°/…/0°/90°] and [90°/0°/…/90°/0°] laminates, however, a substantial deviation was observed in the [90°/0°/0°/90°] laminate with [90°] lamina at the compression side.

탄소섬유 강화 플라스틱 재료의 굽힘시의 이방성 해석

염 영 진
기 계 공 학 과
(1982. 10. 30 접수)

〈要　約〉

탄소섬유 강화플라스틱 재료를 층층이 쌓은 다층적층판과 옆으로 쌓은 적층판에 대한 중립축의 위치를 이론적으로 구하였다.

일축방향 [0°]와 [90°] 단층판에 대한 탄성계수의 측정결과 [0°] 단층판에서는 인장시의 탄성계수가 압축시의 탄성계수보다 31% 더 컸고 [90°] 단층판에서는 7% 더 작았다.

다층 적층판의 중립축의 위치는 변형도 측정에 의해 실험적으로 구해졌다.

중립축 위치의 실험치와 이론치가 비교되었는데 [0°/90°/90°/0°], [0°/90°/…/0°/90°], [90°/0°/…/90°/0°] 적층판에서는 h_t/h의 퍼센트 편차가 3% 이내였으나 [90°] 단층판이 압축하중을 받는 [90°/0°/0°/90°] 적층판에서는 15.3%라는 큰 편차가 나타났다.

Nomenclature

E: modulus
E_t: tensile modulus
E_c: compressive modulus
F: Force
h: beam thickness
h_t: height of tensile zone
h_c: height of compressive zone
N: neutral axis
σ: normal stress
ε: normal strain
ρ: radius of curvature

superscript

(k): No. of layer

I. Introduction

The advantage of composite lamina over conventional materials is that the directional dependence of strength and stiffness of material can be controlled to match the loading direction of structure, reducing its inherent anisotropy of constituent lamina.

The estimation of neutral axis is an important design consideration to the structural engineer because composites are frequently used in flexural mode.

Generally the neutral axis in anisotropic material is not located at the middle plane of symmetry, unlike in the isotropic material due to inequality of tensile and compressive moduli. However, little work has been found in the open literature despite of its serious engineering implication. The work of Jones(1) has shown that the tensile modulus of unidirectional carbon fibre/epoxy composites is 40% greater than compressive modulus while Piggott and Harris(2), by testing unidirectional carbon fibre/polyester reported less rigid in compression than in tension.

In a recent work(3) the authors have reported that the compressive zone decreased with increasing the strain rate during 3-pt. flexural tests of unidirectional carbon fibre/epoxy lamina by direct SEM observation of fracture surface.

This work presents the results of experimentally determined location of neutral axes in [0°/90°/90°/0°] [90°/0°/0°/90°] [0°/90°/…/0°/90°] and [90°/0°/…/90°/0°] laminates.

These results have been compared with a theoretical estimation which is presented in the following.

Theoretical estimation of neutral axis in the edgewise laminates has been also made.

II. Theoretical Analysis

The location of neutral axis in bimodulus composite beam during bending is shown in Fig. (1) as dashed line, where h_c and h_t denote the heights of compressive and tensile zones respectively.

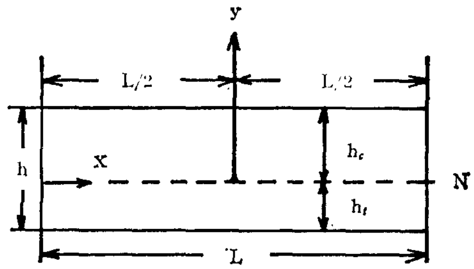

Fig. (1) Location of Neutral Axis

Resultant force at any crosssection of a beam for unit depth is

$$\Sigma F_x=\int_{-h_t}^{h_c}\sigma\,dy=\int_{-h_t}^{0}\sigma_t dy+\int_{0}^{h_c}\sigma_c dy=0 \qquad ①$$

Eq. ① will be used in the following section to calculate the locations of neutral axes in the multilayered and edgewise laminates.

Chamis(4) has shown a theoretical analysis regarding the location of neutral axis in the material having different moduli in tension and compression.

1. Multilayered Laminate

In the arbitrary multilayered laminates the location of neutral axis is obtained as follows.

Assuming the neutral axis is located at the distance x from the bottom of k-th layer of the beam, and each layer has the same thickness of $\frac{h}{n}$, then, from eq. ①

$$\Sigma F_x=\int_{-\frac{k-1}{n}h-x}^{\frac{n-k+1}{n}h-x}\sigma dy=\int_{-\frac{k-1}{n}h-x}^{0}\sigma_t dy+\int_{0}^{\frac{n-k+1}{n}h-x}\sigma_c dy=0 \qquad ②$$

The stress distribution in each layer is

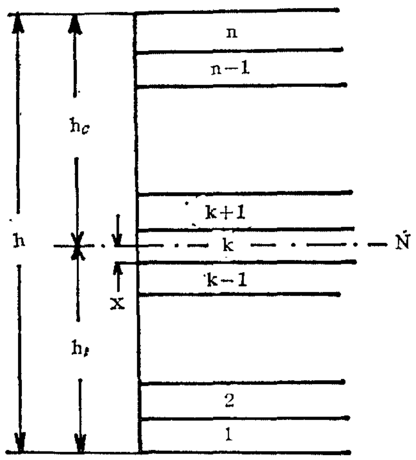

Fig. (2) Neutral axis in multilayered laminate

$$\sigma_t^{(1)} = E_t^{(1)}\varepsilon_t^{(1)} = E_t^{(1)}\left(-\frac{y}{\rho}\right)^{(1)}$$

$$-\frac{k-1}{n}h-x\leq y\leq -\frac{k-2}{n}h-x$$

$$\sigma_t^{(2)} = E_t^{(2)}\varepsilon_t^{(2)} = E_t^{(2)}\left(-\frac{y}{\rho}\right)^{(2)}$$

$$-\frac{k-2}{n}h-x\leq y\leq -\frac{k-3}{n}h-x$$

$$\vdots$$

$$\sigma_t^{(k)} = E_t^{(k)}\varepsilon_t^{(k)} = E_t^{(k)}\left(-\frac{y}{\rho}\right)^{(k)} \qquad -x\leq y\leq 0$$

$$\sigma_c^{(k)} = E_c^{(k)}\varepsilon_c^{(k)} = E_c^{(k)}\left(-\frac{y}{\rho}\right)^{(k)} \qquad 0\leq y\leq \frac{h}{n}-x$$

$$\vdots$$

$$\sigma_c^{(n)} = E_c^{(n)}\varepsilon_c^{(n)} = E_c^{(n)}\left(-\frac{y}{\rho}\right)^{(n)}$$

$$\frac{n-k}{n}h-x\leq y\leq \frac{n-k+1}{n}h-x$$

Substituting these stresses into eq. ② and integrating yields

$$\sum_{m=1}^{k-1}\left\{\frac{h^2}{n^2}[2(k-m)-1]+\frac{2hx}{n}\right\}E_t^{(m)}+E_t^{(k)}x^2$$
$$=\sum_{l=k+1}^{n}\left\{\frac{h^2}{n^2}[2(l-k)+1]-\frac{2hx}{n}\right\}E_c^{(l)}$$
$$+E_c^{(k)}\left(\frac{h}{n}-x\right)^2 \qquad ③$$

From this equation, the location of neutral axis in the multilayered laminate can be obtained as

$$h_t=\frac{k-1}{n}h+x \qquad ④$$

2. Edgewise laminate

(1) Two-layered edgewise laminate

It is assumed that each of the two layers has the same width.

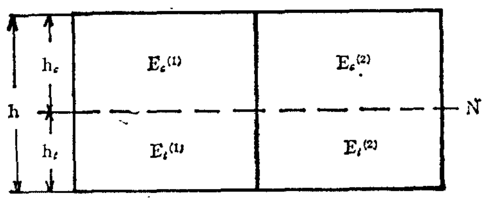

Fig. (3) Neutral axis in two-layered edgewise laminate

From eq. ①

$$\Sigma F_x=\int_{-h_t}^{0}\left(-\frac{y}{\rho}\right)E_t^{(1)}dy+\int_{-h_t}^{0}\left(-\frac{y}{\rho}\right)E_t^{(2)}dy$$
$$+\int_{0}^{h_c}\left(-\frac{y}{\rho}\right)E_c^{(1)}dy+\int_{0}^{h_c}\left(-\frac{y}{\rho}\right)E_c^{(2)}dy=0$$

$$\left(E_t^{(1)}+E_t^{(2)}\right)h_t=\left(E_c^{(1)}+E_c^{(2)}\right)h_c$$

$$\therefore\ \frac{h_t}{h}=\frac{E_c^{(1)}+E_c^{(2)}}{E_t^{(1)}+E_t^{(2)}+E_c^{(1)}+E_c^{(2)}} \qquad ⑤$$

(2) Multilayered edgewise laminate

It is also assumed that each layer of the n layered laminate has the same width.

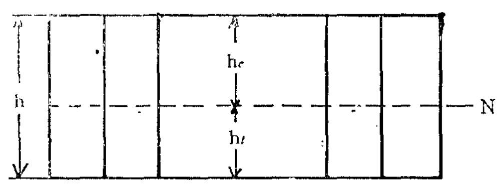

Fig. (4) Neutral axis in multilayered edgewise laminate

From eq. ①

$$\Sigma F_x=\int_{-h_t}^{0}\left(-\frac{y}{\rho}\right)E_t^{(1)}dy+\int_{-h_t}^{0}\left(-\frac{y}{\rho}\right)E_t^{(2)}dy+$$
$$\cdots+\int_{-h_t}^{0}\left(-\frac{y}{\rho}\right)E_t^{(n)}dy$$
$$+\int_{0}^{h_c}\left(-\frac{y}{\rho}\right)E_c^{(1)}dy+\int_{0}^{h_c}\left(-\frac{y}{\rho}\right)E_c^{(2)}dy+\cdots$$
$$+\int_{0}^{h_c}\left(-\frac{y}{\rho}\right)E_c^{(n)}dy=0$$

$$\left(E_t^{(1)}+E_t^{(2)}+\cdots+E_t^{(n)}\right)h_t$$

$$= \left(E_c^{(1)} + E_c^{(2)} + \cdots + E_c^{(n)}\right) h_c$$

$$\therefore \frac{h_t}{h}$$

$$= \frac{E_c^{(1)} + E_c^{(2)} + \cdots + E_c^{(n)}}{E_t^{(1)} + E_c^{(1)} + E_t^{(2)} + E_c^{(2)} + \cdots + E_t^{(n)} + E_c^{(n)}}$$

$$= \frac{\sum_{i=1}^{n} E_c^{(i)}}{\sum_{i=1}^{n} [E_t^{(i)} + E_c^{(i)}]} \quad ⑥$$

Ⅲ. Experiment

1. Specimen Preparation

The nominal one ply thickness of prepreg was 0.16mm and to make a laminate of 50% fibre volume fraction, 20 plies of prepregs were necessary to fill the cavity of the matching mould with the plunger fully closed.

The loaded mould was placed in a preheated press, the plattens of which were thermostatically controlled to 170°C. After waiting for the chosen dwelling time(5)the mould was pressed with a pressure of 50kg/cm² and left to cure for one hour. After this the mould was postcured with the atmospheric pressure at the same temperature for three hours. After postcuring the mould was removed and allowed to cool before extracting the specimen.

2. Bending Test

3-pt. bending is the general method of bending test, however, it is known that the local stress concentration at loading noses during 4-pt. bending is less than that during 3-pt. bending.

The maximum top surface strain and maximum bottom surface strain were measured by 4-pt. bending using two strain gages with the crosshead speed, 0.5mm/min for CFRP regular antisymmetric cross-ply laminates-[0°/90°/…/0°/90°] [90°/0°/…/90°/0°] and regular symmetric crossply laminates-[0°/90°/90°/0°] [90°/0°/0°/90°].

Ⅳ. Results and Discussion

The tensile moduli of [0°] and [90°] unidirectional CFRP laminae were experimentally determined as 34.12GN/m² and 8.34GN/m² respectively. The compressive moduli of these laminae were obtained from tensile moduli and the equation presented by Chamis.(4) As a result, the compressive moduli of [0°] and [90°] laminae were 26.0GN/m² and 8.96GN/m² respectively.

$E_t/E_c = 1.31$ of [0°] lamina, which is somewhat less than the value of $E_t/E_c = 1.4$ reported by Jones(1), however, this shows an apparent

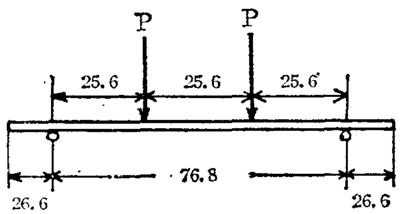

(a) 4-pt. bending

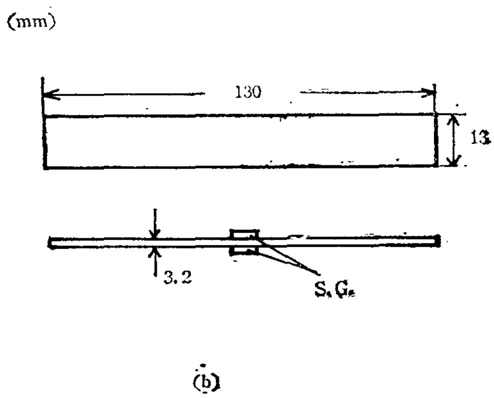

(b) Bending specimen

Fig. (5) Bending Test

difference between the tensile and result compressive moduli. And it is to be noted that for a [90°] lamina, compressive modulus is 7% greater than tensile modulus.

The theoretical estimation of neutral axis in multilayered laminates which was presented in the preceeding section, and experimentally determined values are compared in Table(I), in terms of h_t/h, where h_t denotes the height of tensile zone, and h, the thickness of the beam.

Table. (1) Comparison of theoretical and experimentally determined h_t/h of laminates.

Stacking Sequence	Experimental h_t/h	Theoretical h_t/h	Deviation of h_t/h (%)
[0°/90°/90°/0°]	0.458	0.462	0.9
[90°/0°/0°/90°]	0.425	0.490	15.3
[0°/90°/…/0°/90°]	0.481	0.490	1.9
[90°/0°/…/90°/0°]	0.471	0.457	3.0

It is interesting to note that the percentage deviations of h_t/h in the [0°/90°/90°/0°] [0°/90°/…/0°/90°] and [90°/0°/…/90°/0°] laminates were shown to be less than 3%, while [90°/0°/0°/90°] laminate with [90°] lamina at the compression tended to show larger deviation 15.3%.

Ⅴ. Conclusion

CFRP [0°] and [90°] laminae showed a great anisotropy, showing tensile moduli to be 31% greater and 7% less than compressive moduli for [0°] and [90°] laminae respectively.

Consequently the location of neutral zone in the CFRP laminates shifts from the geometrical center line according to the ratio of compressive and tensile moduli of each layer.

Theoretical estimation of the neutral axis has been made for multilayered laminates. This prediction has been compared with experimental results of laminates having various stacking sequences. — [0°/90°/90°/0°] [90°/0°/0°/90°] [0°/90°/…/0°/90°] and [90°/0°/…/90°/0°] laminates.

The experimentally determined location of neutral axis in the laminates are in good agreement with those of theoretically predicted location except [90°/0°/0°/90°] laminate, where the [90°] lamina was subjected to the compressive load.

Theoretical estimation of the neutral axis has been made for edgewise laminates, too.

References

1. Jones, R.M. ; Stress-Strain Relations for Materials with Different Moduli in Tension and Compression, AIAA Journal, p.16, No.1, Vol.15, 1977.
2. Piggott, M.R. and Harris, B. ; Compression Strength of Carbon, Glass and Kevla-49 Fibre Reinforced Polyester Resin, J. Materials Science, 15, 2523, 1980.
3. Kimpara, I., Kim, H.C., Oshawa, I., and Takebana, ; Fractography of Unidirectional CFRP under Three Point Bending, Journal of Society of Material Science, Japan, 28, 1160, 1979.
4. Chamis, C.C. ; Analysis of the Three-Point-Bend Test for Materials with Unequal Tension and Compression Properties, Proc., 29th Ann. Tech. Conf., SPI. Sec.16-D, 1974.
5. Thompson, S.C., Kim, H.C. and Matthew, F.L. ; The Effect of Processing on the Microstructure of CFRP, Composite, 86, March, 1973.